Local electric field enhancement and polarization effects in a surface-enhanced Raman scattering fiber sensor with chessboard nanostructure

Shuqi Chen[1,2,3*], Lin Han[1,3], Axel Schülzgen[1], Hongbo Li[1,2], Li Li[1], Jerome V. Moloney[2], and N. Peyghambarian[1]

[1]*College of Optical Sciences, The University of Arizona, Tucson, Arizona 85721, USA*
[2]*Arizona Center for Mathematical Sciences, The University of Arizona, Tucson, Arizona 85721, USA*
[3]*Photonics Center, College of Physics, Nankai University, Tianjin 300071, China*
[*]*Corresponding author: schen@optics.arizona.edu*

Abstract: A surface-enhanced Raman scattering fiber sensor with chessboard nanostructure on a cleaved fiber facet is studied by finite-difference time-domain method. Surface plasmons at the metal coated nanostructured fiber facet can be effectively excited and strong local electric field enhancement is obtained. Studies on the influence of light polarization demonstrate a large polarization dependence of the field enhancement factor while the polarization effects on the plasmon resonance wavelength are relatively small.

OCIS codes: (060.4005) Microstructured fibers; (060.2370) Fiber optics sensors; (300.6450) Spectroscopy, Raman; (280.1415) Biological sensing and sensors.

References and links

1. K. Kneipp, Y. Wang, H. Kneipp, L. T. Perelman, I. Itzkan, R. R. Dasari, and M. S. Feld, "Single Molecule Detection Using Surface-Enhanced Raman Scattering (SERS)," Phys. Rev. Lett. **78**, 1667-1670 (1997).
2. S. M. Nie and S. R. Emory, "Probing Single Molecules and Single Nanoparticles by Surface-Enhanced Raman Scattering," Science **275**, 1102-1106 (1997).
3. H. X. Xu, E. J. Bjerneld, M. Käll, and L. Börjesson, "Spectroscopy of Single Hemoglobin Molecules by Surface Enhanced Raman Scattering," Phys. Rev. Lett. **83**, 4357-4360 (1999).
4. V. P. Safanov, V. M. Shalaev, V. A. Markel, Y. E. Danilova, N. N. Lepeshkin, W. Kim, S. G. Rautian, and R. L. Armstrong, "Spectral Dependence of Selective Photomodification in Fractal Aggregates of Colloidal Particles," Phys. Rev. Lett. **80**, 1102-1105 (1998).
5. K. Kneipp, H. Kneipp, P. Corio, S. D. M. Brown, K. Shafer, J. Motz, L. T. Perelman, E. B. Hanlon, A. Marucci, G. Dresselhaus, and M. S. Dresselhaus, "Surface-Enhanced and Normal Stokes and Anti-Stokes Raman Spectroscopy of Single-Walled Carbon Nanotubes," Phys. Rev. Lett. **84**, 3470-3473 (2000).
6. D. H. Murgida and P. Hildebrandt, "Proton-Coupled Electron Transfer of Cytochrome c," J. Am. Chem. Soc. **123**, 4062-4068 (2001).
7. D. L. Stokes, Z. H. Chi, and T. Vo-Dinh, "Surface-Enhanced-Raman-Scattering-Inducing Nanoprobe for Spectrochemical Analysis," Appl. Spectrosc. **58**, 292-298 (2004).
8. A. Lucotti and G. Zerbi, "Fiber-optic SERS sensor with optimized geometry," Sens. Actuators B **121**, 356-364 (2007).
9. A. Lucotti, A. Pesapane, and G. Zerbi, "Use of a Geometry Optimized Fiber-Optic Surface-Enhanced Raman Scattering Sensor in Trace Detection," Appl. Spectrosc. **61**, 260-268 (2007).
10. Y. Zhang, C. Gu, A. M. Schwartzberg, and J. Z. Zhang, "Surface-enhanced Raman scattering sensor based on D-shaped fiber," Appl. Phys. Lett. **87**, 123105-1-3 (2005).
11. H. Y. Chu, Y. Liu, Y. Huang, and Y. Zhao, "A high sensitive fiber SERS probe based on silver nanorod arrays," Opt. Express **15**, 12230-12239 (2007).
12. C. Gu, Y. Zhang, A. M. Schwartzberg, and J. Z. Zhang, "Ultra-sensitive Compact Fiber Sensor Based on Nanoparticle Surface Enhanced Raman Scattering," Proc. of SPIE **5911**, 591108-1-11 (2005).
13. S. O. Konorov, C. J. Addison, H. G. Schulze, R. F. B. Turner, and M. W. Blades, "Hollow-core photonic crystal fiber-optic probes for Raman spectroscopy," Opt. Lett. **31**, 1911-1913 (2006).

#97173 - $15.00 USD Received 10 Jun 2008; revised 23 Jul 2008; accepted 23 Jul 2008; published 11 Aug 2008

14. Y. Zhang, C. Shi, C. Gu, L. Seballos, and J. Z. Zhang, "Liquid core photonic crystal fiber sensor based on surface enhanced Raman scattering," Appl. Phys. Lett. **90**, 193504-1-3 (2007).
15. F. M. Cox, A. Argyros, M. C. J. Large, and S. Kalluri, "Surface enhanced Raman scattering in a hollow core microstructured optical fiber," Opt. Express **15**, 13675-13681 (2007).
16. A. V. Whitney, B. D. Myers, and R. P. V. Duyne, "Sub-100 nm Triangular Nanopores Fabricated with the Reactive Ion Etching Variant of Nanosphere Lithography and Angle-Resolved Nanosphere Lithography," Nano Lett. **4**, 1507-1511 (2004).
17. W. Srituravanich, N. Fang, C. Sun, Q. Luo, and X. Zhang, "Plasmonic Nanolithography," Nano Lett. **4**, 1085-1088 (2004).
18. M. Kahl, E. Voges, S. Kostrewa, C. Viets, and W. Hill. "Periodically structured metallic substrates for SERS," Sens. Actuators B **51**, 285-291 (1998).
19. A. Dhawan and J. F. Muth, "Engineering surface plasmon based fiber-optic sensors," Mater. Sci. Eng. B **149**, 237-241 (2008).
20. A. Dhawan and J. F. Muth, "Plasmon resonances of gold nanoparticles incorporated inside an optical fibre matrix," Nanotechnology **17**, 2504-2511 (2006).
21. A. Dhawana, Y. Zhang, F. Yan, M. Gerholda, and T. Vo-Dinh, "Nano-engineered surface-enhanced Raman scattering (SERS) substrates with patterned structures on the distal end of optical fibers," Proc. of SPIE **6869**, 68690G-1-10 (2008).
22. D. J. White and P. R. Stoddart, "Nanostructured optical fiber with surface-enhanced Raman scattering functionality," Opt. Lett. **30**, 598-600 (2005).
23. M. Moskovit, "Surface-enhanced Raman spectroscopy: a brief retrospective," J. Raman Spectrosc. **36**, 485-496 (2005).
24. Y. Liu, J. Fan, Y. P. Zhao, S. Shanmukh and R. A. Dluhy, "Angle dependent surface enhanced Raman scattering obtained from a Ag nanorod array substrate," Appl. Phys. Lett. **89**, 173134-3 (2006).
25. T. Itoh, K. Hashimoto, and Y. Ozaki, "Polarization dependences of surface plasmon bands and surface-enhanced Raman bands of single Ag nanoparticles," Appl. Phys. Lett. **83**, 2274-2276 (2003).
26. J. M. McLellan, Z. Y. Li, A. R. Siekkinen, and Y. Xia, "The SERS Activity of a Supported Ag Nanocube Strongly Depends on Its Orientation Relative to Laser Polarization," Nano Lett. **7**, 1013-1017 (2007).
27. F. J. García-Vidal and J. B. Pendry, "Collective Theory for Surface Enhanced Raman Scattering," Phys. Rev. Lett. **77**, 1163-1166 (1996).

1. Introduction

Surface-enhanced Raman scattering (SERS) opens up exciting opportunities in the fields of vibrational spectroscopy of chemical and biological objects. SERS can provide ultrasensitive detection [1-3] and extremely high spatial resolution [4-5] and even combine both features for identification of molecules as well as detailed studies of chemical and biological processes [6]. In the last few years, there has been a lot of interest in developing the SERS sensors based on optical fiber. Examples include angled tip fiber sensor [7-9], D-shaped fiber sensor [10-11], nanorod arrays fiber sensor [12], and hollow core photonic crystal fiber [13-15]. Using optical fibers as a SERS platform provides a number of advantages. First, optical alignment is easy and the confinement of light to the fiber core is assured once the light is coupled into the fiber. Second, the detection location is well-defined and easy to control. Third, there are a number of ways to make the SERS active surfaces on the fiber tip, including UV lithography, nanosphere lithography, e-beam lithography, and focused ion beam (FIB) [16-19].

Recently, there has been particular interest in the use of patterned structures on the distal end of SERS fiber sensors [19-22]. Patterned structures have been fabricated by lithography, FIB method or chemical methods and many different patterns can be realized. Often, the parameters of the fabricated structures and structures are chosen rather arbitrarily in previous papers [19-21]. As a result, the resonance wavelength of the nanostructures is not consistent with the pump wavelength and, therefore, the pump light may not couple efficiently to intrinsic plasmon excitations of the nanostructures.

The large variety of possible structures combined with time and effort to be spent in fiber nanostructure fabrication emphasizes the utility of appropriate theoretical studies with predictive capability. For instance, while the important role played by polarization in the SERS process has been recognized in the case of nanoparticles, such as nanorods and nanocubes [2, 12, 23-26], to the best of our knowledge it has not been studied for SERS

#97173 - $15.00 USD Received 10 Jun 2008; revised 23 Jul 2008; accepted 23 Jul 2008; published 11 Aug 2008

sensors with patterned fiber facets. Polarization effects will certainly be also important to understand the local field enhancement on fiber facets with embedded nanostructures.

In this paper, we present a novel design of a SERS fiber sensor with a chessboard nanostructure that could be fabricated on the tip of an optical fiber. Electromagnetic fields and local field enhancement is studied theoretically using a three-dimensional finite-difference time-domain (FDTD) algorithm. With our study we try to accommodate the need for an optimization process for fiber integrated SERS sensors. We demonstrate that in the proposed chessboard structure surface plasmon (SP) excitation is very effective and strong local field enhancement can be achieved. We also study and show the impact of polarization effects on the SERS enhanced factor and the SP resonance.

2. Structure and simulation

The basic geometry of chessboard nanostructure on the distal end of optical fiber is shown in Fig. 1(a), and Fig. 1(b) shows a top view of a unit cell of the simulated structure. A nanoscale chessboard landscape could be fabricated at the tip of an optical fiber by lithography and chemical etching or FIB. After nanofabrication the fiber tip should be coated with gold. The planar scale (side length of each square) and the thickness of the gold layer are about several hundred nanometers and ten nanometers, respectively. We assume that there are many unit cells fabricated at the position of the core of a multimode optical fiber. Most likely there will be a little overlap between adjacent squares, a fact that we would define as a negative gap in our simulation.

The polarization effects and SP resonance of the SERS chessboard nanostructure sensor is studied through three-dimensional FDTD electromagnetic simulations, using spatial mesh size of 1 nm or 2 nm along the x and y directions, and 2 nm along the z direction. The total simulation volume is the area of a unit cell equal to 2(Length+Gap)×2(Length+Gap) (see Fig. 1(b)) times 400 nm in the z direction. The incident pump light propagating in z direction is generated by a total field/scattering field technique. Perfectly matched layers (PML) are used at the top and bottom of the simulation domain to completely absorb waves leaving the simulation domain in the direction of propagation. Periodic boundary conditions are used in the x-y directions. The permittivity of gold is expressed by a modified Deybe model which agrees well with experimental data in the spectral region between 600 nm and 1100 nm. The polarization of the pump light is defined as the angle φ with the x-axis in the x-y plane. To determine the local intensity enhancement, we set four monitoring points as illustrated in Fig. 1(b), which are at the top surface of the gold.

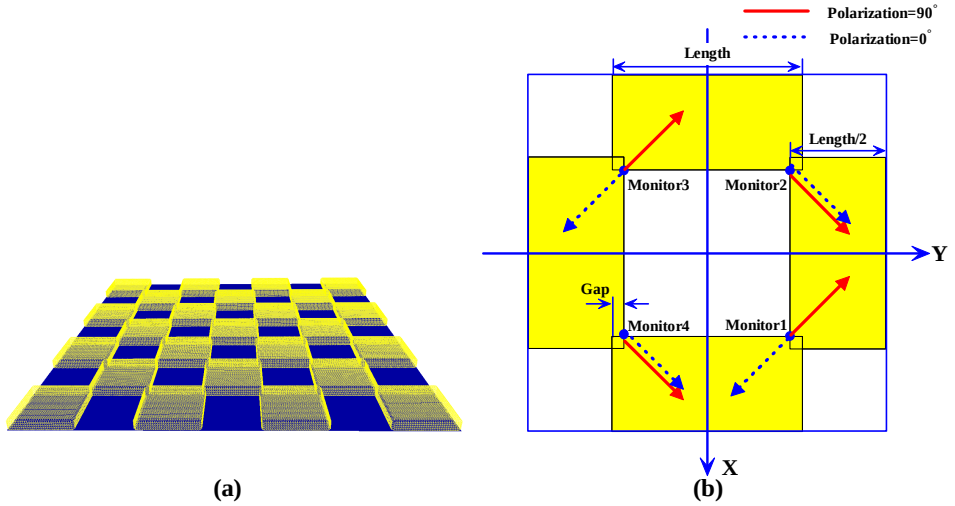

Fig. 1. (a). The basic geometry of chessboard nanostructure on the distal end of optical fiber. (b). The simulated structure viewed from the top.

#97173 - $15.00 USD Received 10 Jun 2008; revised 23 Jul 2008; accepted 23 Jul 2008; published 11 Aug 2008

A single mode fiber only supports two degenerate fundamental HE_{11} modes, or LP_{01} modes. Different superpositions of the two modes can lead to almost linearly polarized (LP) fields (modes) with arbitrary polarization directions or elliptically polarized modes. A unit cell in our chessboard structure has a size of about 200 nm in the transverse directions, which is much smaller than the mode field diameter of a typical single mode fiber, e.g., about 10 micrometers for SMF-28. So a unit cell sees a HE_{11} mode or any combination of two HE_{11} modes like a plane wave with different polarizations. In our simulation, our incident field is a plane wave with a specific polarization. As a result, we can analyze a single unit cell with periodic boundary condition for the lateral boundaries. The situation becomes more complicated for multimode fibers, which support higher order modes, such as TM, TE, EH, and higher order HE modes. For weakly guiding multimode fibers, these aforementioned modes can form higher order LP modes. If a LP mode of a multimode fiber is incident on the chessboard structure, the incident field can again be simplified as a plane wave. In this case, the beam size is even larger, and the plane wave assumption holds even better.

3. Results and discussion

In the first simulation a 785 nm plane wave linearly polarized at a 45° angle with respect to the x-axis was launched in the +z direction. Near infrared excitation by a 785 nm semiconductor laser is often used in vibrational molecule spectroscopy due to its limited damage to molecules. In order to make our simulation practical, we varied the length of the chessboard squares to keep the plasmon resonance at 785 nm. When the chessboard structure is resonantly excited, the electric field localization around the gap is maximized. Figure 2 gives the normalized electric field intensity for the chessboard nanostructure fiber sensor, where the length, thickness and gap of the chessboard geometry are 108 nm, 10 nm and 0, respectively. In this case, the spatial mesh sizes are 1 nm in both x and y directions. We can see that the SP can be effectively excited and strongly enhanced electric field is obtained in this sensor. Moreover, there are only two peaks at monitor 2 and monitor 4. It is because the electric field is in phase at monitors 2 and 4 when the polarization of the incident light is 45°. However, it is out of phase at monitors 1 and 3. Figure 1(b) indicates the electric field vectors for different monitor positions.

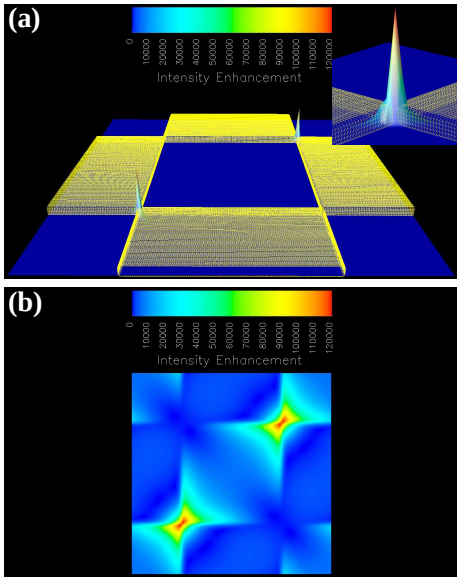

Fig. 2. (a). The intensity enhancement distribution for the chessboard nanostructure. Inset: the largest intensity enhancement. (b). The intensity enhancement distribution at the top surface of the chessboard nanostructure.

#97173 - $15.00 USD Received 10 Jun 2008; revised 23 Jul 2008; accepted 23 Jul 2008; published 11 Aug 2008

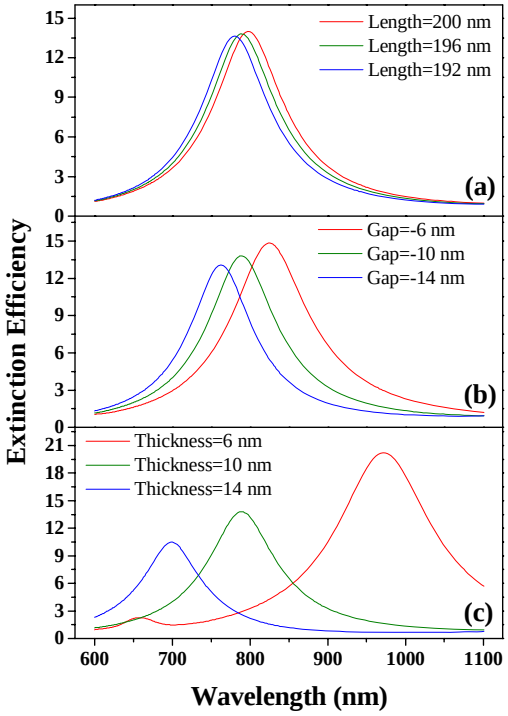

Fig. 3. The extinction spectra of the chessboard nanostructure. (a). Gap=-10 nm, Thickness=10 nm; (b). Length=196 nm, Thickness=10 nm; (c). Length=196 nm, Gap=-10 nm;

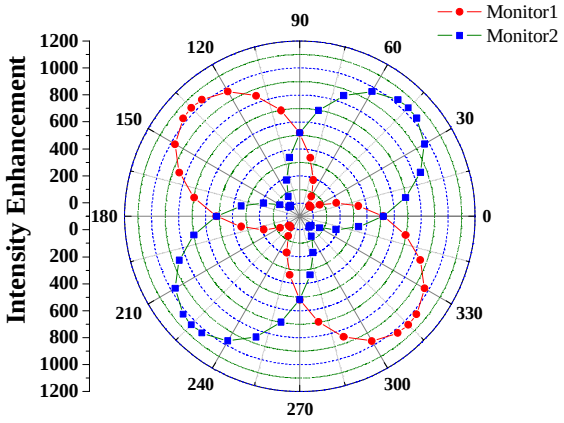

Fig. 4. The polarization effects on local field enhancement at different monitor positions in a polar diagram.

To a first approximation, the electromagnetic enhancement factor G_{SERS} can be expressed by the fourth power of the ratio of the total electric field $E(r_m, \upsilon)$ at the molecule location r_m to the incident excitation field $E_{inc}(\upsilon)$, where υ is the laser frequency [27]. The calculations

#97173 - $15.00 USD Received 10 Jun 2008; revised 23 Jul 2008; accepted 23 Jul 2008; published 11 Aug 2008

indicate that the maximum theoretical electromagnetic enhancement factor can reach almost 10^{10} in our chessboard nanostructure fiber sensor.

Next we studied the effect of several structural parameters on the resonance wavelength. The spatial mesh sizes are set to 2 nm in the x and y directions and the gap is -10 nm in the following simulations. Figure 3 shows the extinction spectra of several chessboard structures with different lengths (Fig. 3(a)), gaps (Fig. 3(b), and thicknesses (Fig. 3(c)). The incident light is a 5 fs (FWHM) Gaussian pulse with a central wavelength of 785 nm. The extinction spectra are obtained by the Fourier transforming both the incident and transmitted pulses. The plasmon resonance wavelength (maximum extinction) is exactly 785 nm when the length, thickness, and gap are 196 nm, 10 nm, and -10 nm, respectively. We can see that the resonance shifts to longer wavelength with increasing length or increasing negative gap size corresponding to a larger overlap between adjacent gold squares. Decreasing the gold layer thickness also results in a red shift and the influence of the thickness to the resonant wavelength is in fact larger than that of the other parameters. Meanwhile, the extinction efficiency will slightly increase with increasing length or decreasing gap or thickness. The higher the extinction efficiency, the more efficient is the SP excitation.

Previous investigations of polarization effects on nanorods and nanocubes [24, 26] indicated that the polarization of the incident light plays an important role in the SERS process. Therefore, to optimize the electromagnetic enhancement factor, one must take into account the vectorial nature of the fields involved. The intensity enhancement at 785 nm for different incident linear polarizations is shown in Fig. 4. Again, the magnitude of the intensity enhancement is obtained by the Fourier transform method as in Fig. 3. Results show that the intensity enhancement of monitor 1 and monitor 2 reach minimum or maximum values when the incident light is polarized along the diagonal of the chessboard structure. However, the intensity enhancement of monitor 1 and monitor 2 are equal and about half of the maximum value when the incident light is polarized along the x-axis or y-axis. Although there are twice as many positions of the highest local field enhancement when the polarization is 0° compared to a 45° polarization, one should choose 45° polarization and maximum enhancement to obtain the largest SERS signal. The maximum electromagnetic enhancement factor is determined by the largest SERS signal.

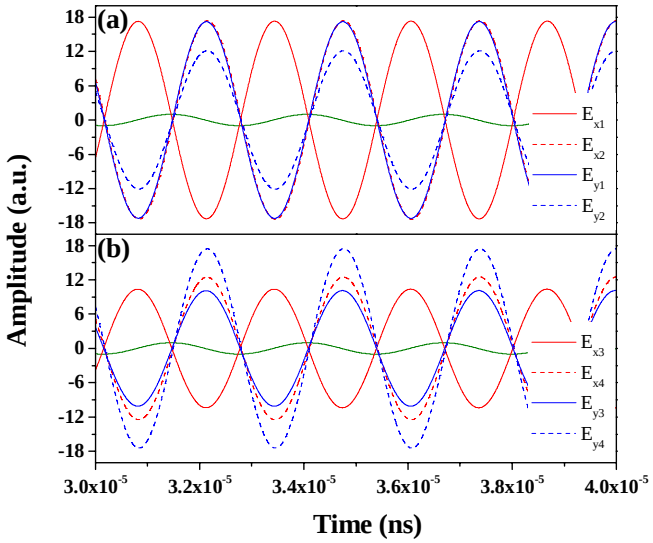

Fig. 5. The time history of electric field for different monitors when the polarization is 90°. The olive line represents propagation in the vacuum. (a). Monitor 1 and monitor 2; (b). Monitor 3 and monitor 4;

#97173 - $15.00 USD Received 10 Jun 2008; revised 23 Jul 2008; accepted 23 Jul 2008; published 11 Aug 2008

In order to understand the physics behind the polarization effects shown in Fig. 4, we plot the time evolution of the electric fields at different monitor positions after launching 785 nm light polarized along the y-axis. Figure 5 demonstrates that the electric fields at different monitor locations have different phases with respect to the electric field propagating in vacuum. The amplitudes of the local electric fields in Fig. 5 are not absolutely equal to each other. This is a numerical artifact because the mesh in our simulations is not symmetrical regarding the four monitor positions during the auto-meshing process. However, this asymmetry will not influence the respective phases of the local electric fields and the underlying physics. Table 1 lists the phase differences of the electric field for different monitors in the case of an incident 90° linear polarization. Using the listed phase differences, we plot the electric field vectors for different monitor positions as red arrows in Fig. 1(b). We also plot the electric field vectors for an incident polarization of 0° as blue dotted arrows according the symmetry of the chessboard nanostructure. The electric field vectors for the 45° polarized incident field are the linear superposition of the electric fields of the 0° and 90° polarized incident fields. When the polarization is 45°, the electric field of the 0° polarized incident light is out of phase with respect to that of the 90° polarized incident light at monitors 1 and 3, while these fields are in phase at monitors 2 and 4. This explains that the field enhancement shown in Fig. 2 is maximum at monitors 2 and 4.

Table 1. The phase differences of the electric field for different monitors when the polarization is 90°.

Monitor	**Phase difference**	
	$\mathbf{E_x}$	$\mathbf{E_y}$
Monitor 1	$-3\pi/2$	$-\pi/2$
Monitor 2	$-\pi/2$	$-\pi/2$
Monitor 3	$-3\pi/2$	$-\pi/2$
Monitor 4	$-\pi/2$	$-\pi/2$

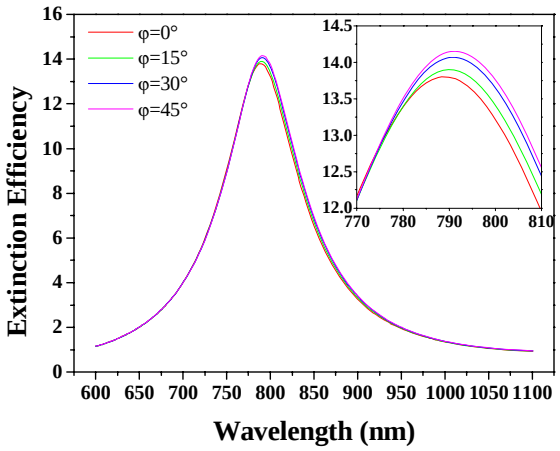

Fig. 6. The extinction spectra of the chessboard nanostructure for different polarizations, where length, gap, and thickness are 196 nm, -10 nm and 10 nm, respectively. Inset: zoom in the extinction spectra around the resonant wavelength.

#97173 - $15.00 USD Received 10 Jun 2008; revised 23 Jul 2008; accepted 23 Jul 2008; published 11 Aug 2008

Figure 6 shows the extinction spectra for different polarizations. Because the chessboard structure has a perfect symmetry and the local field enhancement will repeat every 45° according to Fig. 4, we only need to take into account the polarizations from 0° to 45°. Although the polarization dependence of the maximum intensity enhancement is striking, the polarization effect on the resonance wavelength is almost negligible. Therefore, we don't need to worry about the shift of the resonance wavelength when we adjust the polarization of the incident light to obtain the maximum electromagnetic enhancement factor.

4. Conclusions

In conclusion, we presented a novel chessboard nanostructure design that can be used as an effective SERS fiber sensor when fabricated directly on the tip of an optical fiber. Using FDTD simulations, an effective resonant excitation of SP and strong local field enhancement has been demonstrated. Our studies also showed the dependence on structural parameters and the polarization of incident light. Our results can be used to optimize the nanostructure geometry and understand the polarization properties of the proposed fiber integrated SERS sensor. This work is instructive and brings predictive capabilities to the design of SERS experiment based on nanostructured fiber tips.

Acknowledgments

This work is supported by the National Sciences Foundation (Grant No. 0725479), the state of Arizona TRIF Photonics Initiative, and Air Force Office of Scientific Research (Grand No. FA9550-07-1-0010 and FA9550-04-1-0213).

#97173 - $15.00 USD Received 10 Jun 2008; revised 23 Jul 2008; accepted 23 Jul 2008; published 11 Aug 2008